Rotor Design Optimization of Synchronous Reluctance Machine

Takayoshi Matsuo, *Student Member, IEEE* Thomas A. Lipo, *Fellow, IEEE*

University of Wisconsin-Madison
Electrical and Computer Engineering
1415 Johnson Drive
Madison, Wisconsin 53706

***Abstract*—It is demonstrated that the rotor design of synchronous reluctance machines can be optimized in terms of a key geometric parameter, i.e., the ratio of the rotor insulation width to the rotor iron width so as to obtain maximum torque production. The equation which gives the maximum motor power factor in terms of the saliency ratio has been derived and it is shown that the power factor of 0.8 is a realizable value with the optimal rotor design. An experimental motor has been fabricated and the results of measurements of the motor parameters prove the validity of the rotor design optimization.**

INTRODUCTION

During the past decade ac motor drives have begun to predominate over dc motor drives for most of variable speed applications. For low power applications, with motor power of less than one hundred kilowatts, voltage source transistor inverter fed induction motor drives have been the solution. The squirrel cage induction motor drive has emerged as the ac motor of choice for most applications due to its low cost, simple structure, and overall satisfactory performance.

The induction motor, however, is not an ideal machine for many applications due to its relatively poor efficiency, and due to difficulties associated with controlling torque. In particular, the widely applied field oriented control of induction machines requires some means to compensate rotor resistance variations because controlled motor torque deviates as the motor parameter varies due to motor temperature variations. Numerous studies have been devoted to the issue, i.e., the identification of rotor resistance or rotor time constant [1]. Modern field oriented control of induction machines also requires the use of a position sensor in the torque loop. Although work on eliminating this sensor in order to reduce cost and improve reliability has been actively pursued for some time, a universally satisfactory solution has not been obtained, while alternate ac motor possibilities have been studied for small power drive applications.

93 SM 352-5 EC A paper recommended and approved by the IEEE Electric Machinery Committee of the IEEE Power Engineering Society for presentation at the IEEE/PES 1993 Summer Meeting, Vancouver, B.C., Canada, July 18-22, 1993. Manuscript submitted Dec. 29, 1992; made available for printing May 3, 1993.

PRINTED IN USA

In particular, a permanent magnet motor is generally accepted as the ideal motor in that the machine has the highest efficiency and thus the smallest frame size of all ac motors for power range of less than a few kilowatts. The cost of the magnet material together with the cost of the associated assembly, however, will prevent such machines from assuming its rightful place as the motor of choice for the near future.

Another machine which has been proposed for variable speed drives is the variable reluctance or so-called "switched reluctance" motor. While the concept of the motor can be traced back before 1900, the machine has only been pursued for variable speed drives for about 15 years. This machine relies upon "reluctance torque" rather than the more conventional "reaction torque" of wound field synchronous, surface magnet PM and induction machines. In this machine the stator and rotor have projecting poles along the air gap and torque is produced by the tendency of the rotor to line up along a minimum reluctance position established by the alignment of a particular stator and rotor saliency (i.e., pole). Continuous rotation is produced by sequentially switching the stator current from one phase to the next as the rotor pole moves into alignment with each successive stator pole.

It has gradually been shown that the variable reluctance machine can compete favorably with induction machines, particularly in small sizes below a few kilowatts where the decreasing magnetizing inductance of the induction motor causes performance degradation. Unfortunately, the variable reluctance machine has its own set of problems such as high torque pulsation at low speed, considerable audible noise, cost penalties due to small mechanical tolerances, substantial switch volt-ampere rating, and relatively high losses during the field weakening condition. While much work has been done on addressing these problems it is extremely difficult to find a solution which solves all of them simultaneously. While variable reluctance will undoubtedly find its rightful place in the application spectrum, it does not appear, at this point in time, that such machines will have much of an impact across the board.

Another machine, which has been relatively ignored for the past several decades is the synchronous reluctance motor. This machine can also be traced back to the misty origins of electrical machinery and has been a subject in learned journals for at least seven decades. The synchronous reluctance motor is a singly salient machine in which the rotor is constructed so as to again employ the principle of reluctance torque to produce electromechanical energy conversion. In this case, however, only the rotor is constructed with salient poles while the stator inner surface is cylindrical and typically wound in an identical manner to an induction machine. Thus the machine typically retains many of the benefits of variable reluctance motors while at the same time eliminating several of its disadvantages. The noise and torque pulsation

problems, so difficult to overcome with variable reluctance motors, can be elegantly overcome in a synchronous reluctance machine by simply winding the stator in the conventional manner sc as to produce a sinusoidal uniformly rotating air gap MMF.

PREVIOUS WORK

The synchronous reluctance motor (salient-pole rotor without field coils) is one of the oldest types of electric motors and has, from time to time, attracted the efforts of a considerable number of investigators [2]. Kostko proposed the adoption of a cylindrical rotor with multiple slits along the lines of the direct-axis flux, which is shown in Figure 1 (a) [3]. His work is substantially the basis for the designs of rotors with reluctance slots, flux guides and segments.

In the 1930s, a typical rotor punching was identical to many induction motor punchings except that a few teeth were cut out. A high saliency ratio cannot be expected for this rotor configuration. These motors are generally characterized by very low power factors or efficiencies or both. As a result reluctance motors are larger than induction motors of corresponding rating. Its low weight efficiency and poor performance are inadmissible in motors of larger output and seemed to justify the general opinion that the synchronous reluctance motor is inherently inferior to the other types of ac motors.

The rotor of a "second generation" type of synchronous reluctance motor which appeared somewhat later is shown in Fig. 1 (b) which utilizes a segmental rotor construction [4]. A rotor cage was not used to start the machine, but, rather, the machine was started in synchronism with the inverter frequency. Saliencies of five or more were obtained with such machines which enabled such machine to fit in the same frame size as their induction motor counterpart. Cost, however, was a problem since the rotor segments were constructed either with solid poles or with many small laminations which had to be secured to each other and then bolted on the rotor shaft. However, the poor power factor and efficiency have continued to plague the widespread use of such machines.

A modern "third generation" type of rotor construction is shown in Fig. 1 (c). In this case, the rotor is constructed of axially laminated steel sheets bent into a "u" or "v" shape and then stacked in the radial direction [5]. The analogy to four stacked piles of "rain gutters" to form four poles mounted on a solid shaft can be used to describe the overall shape. In this case the permeance (inductance) in the direction of the gutters form the salient poles (d-axis) while the interpolar axis is formed by flux paths which are normal to the direction of the gutters. Saliencies of seven or more have been reported with this type of structure, which typically results in a machine which competes favorably with an induction motor. The primary difficulty with such a machine is again the high manufacturing cost of the rotor which could, perhaps, be eliminated or at least minimized with mass production.

THE d-q EQUATIONS FOR THE SYNCHRONOUS RELUCTANCE MACHINE

Since the stator winding of the synchronous reluctance machine is sinusoidally distributed, flux harmonics in the air gap contribute only an additional term to the stator leakage inductance. Hence, the equations which describe the behavior of the synchronous reluctance machine can be derived from the conventional equations depicting a conventional wound field synchronous machine, that is Park's Equations. In such machines, the excitation (field) winding is non-existent. Also, in machines typically employing a modern axially laminated rotor structure, a rotor cage is normally omitted since the machine can be started synchronously from rest by proper inverter control. Hence, eliminating both the field winding and damper winding equations from Park's equations forms the basis for the d-q Equations for a synchronous reluctance machine [6]. That is,

$$v_{ds} = r_s\, i_{ds} + \frac{d}{dt} L_{ds}\, i_{ds} - \omega_r\, L_{qs}\, i_{qs} \tag{1}$$

$$v_{qs} = r_s\, i_{qs} + \frac{d}{dt} L_{qs}\, i_{qs} + \omega_r\, L_{ds}\, i_{ds} \tag{2}$$

where L_{ds}, and L_{qs} are, respectively, the direct axis and quadrature axis inductances. The quantity r_s is the stator resistance per phase and ω_r is the speed of the rotor. In terms of the d-q variables, the electromagnetic torque is identical to that of a synchronous machine, namely,

$$T_e = \frac{3}{2}\frac{P}{2}(L_{ds} - L_{qs})\, i_{ds}\, i_{qs} \tag{3}$$

where P is the number of poles.

MAXIMUM POWER FACTOR

A frequently used argument against the use of a synchronous reluctance motor is its "poor" power factor. It is useful to consider this issue more closely. The power factor of a synchronous reluctance motor, cosϕ, can be expressed as the ratio of the projection of the voltage vector on the current vector divided by the amplitude of the voltage vector. That is,

$$\cos\phi = \frac{V_{qs}\sin\varepsilon + V_{ds}\cos\varepsilon}{\sqrt{V_{qs}^2 + V_{ds}^2}} \tag{4}$$

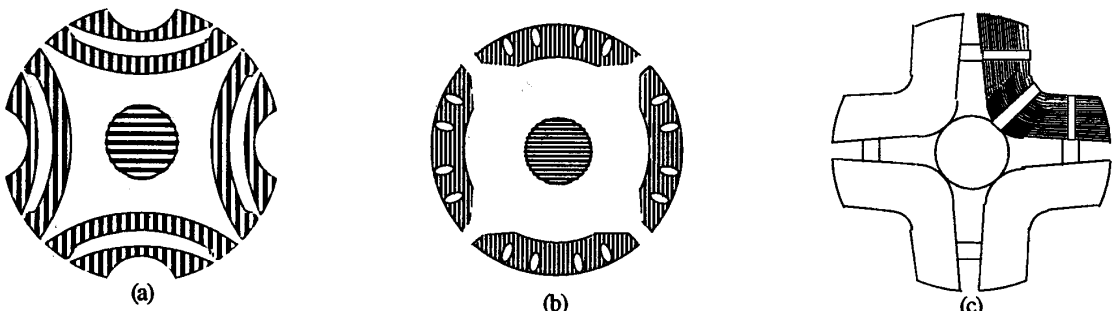

Fig. 1 (a): Kostko's rotor in the 1920s which shows segmental iron pieces and flux barriers. (b): Lawrenson's isolated segmental rotor. (c): General construction of an axially laminated anisotropic rotor.

where V_{ds} and V_{qs} are the d- and q-axis steady state voltage in the rotating reference frame, and ε is the "MMF angle".

Equation 4 gives the power factor as a function of the MMF angle ε. It is useful to determine which value of MMF angle results in the maximum power factor. If this point is chosen as the "rated" value then the machine can be considered as optimally performing its energy conversion function. It can be shown that the power factor reaches a maximum value of

$$\cos\phi_{max} = \frac{\kappa-1}{\kappa+1} k_{\phi max} \tag{5}$$

where

$$k_{\phi max} = \frac{\sqrt{1+\frac{r_s^2}{X_{ds}X_{qs}}}+A}{\sqrt{(1+B)(1+C)}} \tag{6}$$

$$\begin{aligned} A = {} & 2\left(\frac{r_s}{X_{qs}}\right)\left(\frac{1}{\frac{X_{ds}}{X_{qs}}-1}\right)\sqrt{\frac{X_{ds}}{X_{qs}}} \\ & + 2\left(\frac{r_s}{X_{qs}}\right)^2\left(\frac{1}{\frac{X_{ds}}{X_{qs}}-1}\right)\sqrt{1+\frac{r_s^2}{X_{ds}X_{qs}}} \\ & + 2\left(\frac{r_s}{X_{qs}}\right)^3\left(\frac{1}{\frac{X_{ds}}{X_{qs}}-1}\right)\sqrt{\frac{X_{qs}}{X_{ds}}} \end{aligned} \tag{7}$$

$$\begin{aligned} B = {} & 2\left(\frac{r_s}{X_{qs}}\right)\left(1+\frac{r_s^2}{X_{ds}X_{qs}}\right)^{3/2}\left(\frac{1}{\frac{X_{ds}}{X_{qs}}+1}\right)\sqrt{\frac{X_{ds}}{X_{qs}}} \\ & + \left(\frac{r_s}{X_{qs}}\right)^2\left(\frac{1}{\frac{X_{ds}}{X_{qs}}+1}\right)\left(\frac{X_{qs}}{X_{ds}}+3\right) \\ & + 2\left(\frac{r_s}{X_{qs}}\right)^4\left(\frac{1}{\frac{X_{ds}}{X_{qs}}+1}\right)\left(\frac{X_{qs}}{X_{ds}}\right) \end{aligned} \tag{8}$$

$$\begin{aligned} C = {} & 2\left(\frac{r_s}{X_{qs}}\right)\left(\frac{1}{\frac{X_{ds}}{X_{qs}}+1}\right)\sqrt{\frac{X_{ds}}{X_{qs}}}\sqrt{1+\frac{r_s^2}{X_{ds}X_{qs}}} \\ & + 2\left(\frac{r_s}{X_{qs}}\right)^2\left(\frac{1}{\frac{X_{ds}}{X_{qs}}+1}\right) \end{aligned} \tag{9}$$

when the MMF angle reaches

$$\tan\varepsilon = \sqrt{\kappa}\left(\sqrt{1+\frac{r_s^2}{X_{ds}X_{qs}}}+\sqrt{\frac{r_s^2}{X_{ds}X_{qs}}}\right) \tag{10}$$

The motor power factor versus saliency ratio κ ($=L_{ds}/L_{qs}$) under maximum power factor control scheme is plotted in Figure 2, assuming that r_s/X_{ds} is 0.05. Note that for machines with a saliency ratio of 7, the power factor is near 0.8 which is quite typical of a Class B induction machine rated about 10 HP.

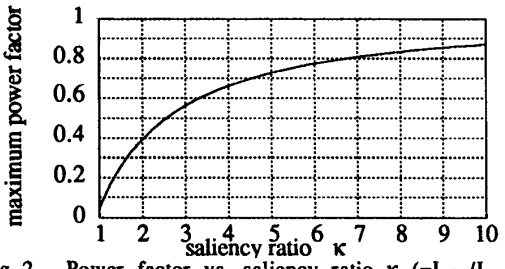

Fig. 2 Power factor vs. saliency ratio κ ($=L_{ds}/L_{qs}$) of a synchronous reluctance motor when the motor is controlled with the maximum power factor control scheme.

ROTOR DESIGN OPTIMIZATION OF SYNCHRONOUS RELUCTANCE MOTOR

The rotor design optimization of the synchronous reluctance motor, which is described in this paper, is based on the optimization of two important factors, i.e., the "motor torque index", (L_{ds}-L_{qs}) and the saliency ratio, L_{ds}/L_{qs}. It is apparent from Eq. 3 that the torque of the synchronous reluctance motor is proportional to the "motor torque index". It is also clear from the discussion above that the motor maximum power factor is dependent upon the saliency ratio, L_{ds}/L_{qs}.

Geometric Parameters

The modern axially laminated four pole configuration of Fig. 3 is assumed. Specifically, the rotor is assumed to be constructed of "packets" of thin laminations which are bent in a semi-circular shape. These thick packets of steel are assumed to be separated by a suitable insulator, perhaps air, but also possibly, plastic laminate or epoxy-like material. All of the lamination segments are assumed to be equally spaced. Also, the machine is assumed to have 24 slots (2 slots/pole/phase) with a tooth width over tooth pitch ratio of 0.54. Figure 4 shows more detail of the rotor construction indicating two key variables, W_{iron} and W_{ins}, corresponding to the width of each rotor segment and of the width of the insulation between segments respectively. The sum of $n(W_{iron} + W_{ins})$ is chosen so as to always equal the width of one stator tooth in order to limit, as much as possible, pulsating fluxes in the stator teeth. In practice, values of n= 1 and 2 were investigated.

For purposes of comparison between different geometries it is useful to define the ratio

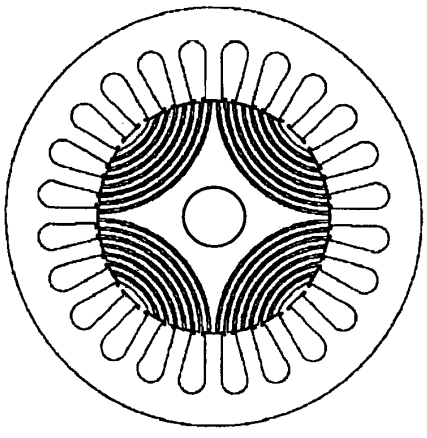

Fig. 3 A synchronous reluctance motor with 24 stator slots.

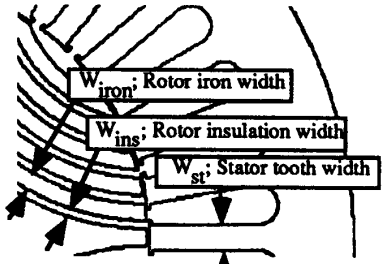

$$W_{st} = (W_{iron} + W_{ins}) \times n$$

where n; integer

Fig. 4 The relation of the stator tooth width W_{st} the rotor iron width W_{iron} and the rotor insulation width W_{ins} for the rotor lamination design of a synchronous reluctance motor.

$$K_W = W_{ins}/W_{iron} \tag{11}$$

Clearly, when $K_W = 0$, the rotor is assumed to be completely made of iron, (i.e., no saliency). When $K_W = 1$ the rotor is constructed of lamination segments in which the air space and lamination segments are equal.

Rotor Design Optimization of Synchronous Reluctance Motor with 24 Stator Slots

Finite element field plots for the two extreme cases of d-axis and q-axis excitation are shown in Figs. 5. Only one-eighth of the machine need be shown due to the symmetry involved. Note that very little flux enters the rotor when the flux is forced to pass through the q-axis. This observation is borne out by examination of Fig. 6 which show the air gap flux density as a function of air gap. In all cases, the surface current density was fixed at 500 A/in resulting in a fairly highly saturated machine.

The d-axis magnetizing inductance L_{md} can be calculated by Equation 12 [7] from the obtained fundamental component of the magnetic flux density B_{g1d}, while the q-axis magnetizing inductance L_{mq} is calculated by Equation 13.

$$L_{md} = \frac{1}{i_{ds}}\left(\frac{k_1 N_1}{N_C}\right)\left(\frac{2}{\pi} B_{g1d}\right)\tau_p l_e \tag{12}$$

$$L_{mq} = \frac{1}{i_{qs}}\left(\frac{k_1 N_1}{N_C}\right)\left(\frac{2}{\pi} B_{g1q}\right)\tau_p l_e \tag{13}$$

where, i_{ds}; d-axis excitation current
i_{qs} q-axis excitation current
k_1; winding factor
N_1; number of turns per phase
N_C; number of circuit in parallel per phase
B_{g1d}; fundamental component of air gap flux density
B_{g1q}; fundamental component of air gap flux density
τ_p; pole pitch
l_e; effective core length

The saliency ratio $K_{saliency}$, which does not include leakage inductance, is expressed as Equation 10 and is the ratio of B_{g1d} to B_{g1q} with the condition of $i_d = i_q$.

$$K_{saliency} = \frac{L_{md}}{L_{mq}} \tag{14}$$

Specifically, for the case of Fig. 6 (a) and (b), the maximum fundamental component of air gap flux for d-axis excitation obtained from a spectral analysis of the wave form is 0.836 while the fundamental component for q-axis excitation is only

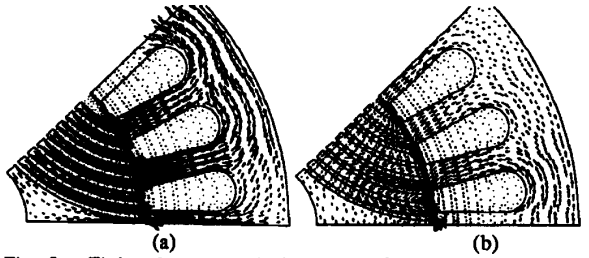

Fig. 5 Finite element analysis results of magnetic flux density distributions of a synchronous reluctance motor with 24 stator slots and K_W (rotor insulation width/ rotor iron width) of 1/2: (a) d-axis excitation, (b) q-axis excitation.

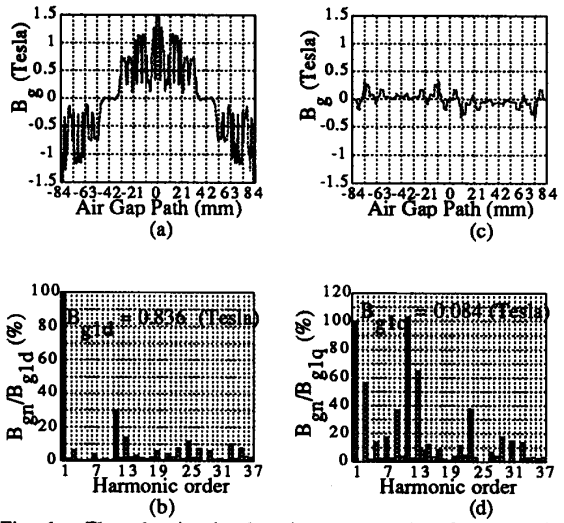

Fig. 6 Flux density in the air gap resulting from the finite element analysis results of a synchronous reluctance motor with 24 stator slots and K_w (rotor insulation width/ rotor iron width) of 1/2: (a) the wave form of the air gap flux density and (b) the harmonic components for d-axis excitation; (c) the wave form of the air gap flux density and (d) the harmonic components for q-axis excitation.

0.084, making the saliency ratio 10 to 1, neglecting the effects of leakage inductance. Since the leakage inductance is on the order of 0.1 per unit, this corresponds to a saliency ratio $\kappa = L_{ds}/L_{qs} \approx 7$ which is still very large.

Figure 7 shows a plot of the saliency ratio $K_{saliency} = L_{md}/L_{mq}$ as a function of K_w. It appears at ratios on the order of 13 or more are achievable with a machine constructed of "real iron", i.e., saturation effects have been included in this study.

While saliency ratio is an important index of merit for a synchronous reluctance machine, examination of Eq. 3 indicates it is the torque per unit power loss or torque per rms amp that defines the effectiveness of any ac machine. Hence, the torque of the synchronous reluctance motor is truly proportional to the difference between the d- and q-axes inductances. Figure 8 shows a plot of L_{md}, L_{mq} and $L_{md} - L_{mq}$ versus the ratio between rotor insulation width and rotor iron width, K_w. Each of the parameters is per unitized to the value of L_{md} for the case of $K_w = 0$ (solid iron rotor).

Note that the maximum value of the difference L_{md}–L_{mq} occurs in the range of K_w between 0.2 and 0.6. In general, it

is desirable to keep K_w as small as possible, since small K_w corresponds to more rotor iron, corresponding to lower flux density and consequently lower iron tooth pulsation losses. On the other hand, the value of K_w cannot be made too small for constructional reasons. Hence, a value on the order of 0.5 appears to be about optimum. The value of $K_{saliency}$ in Fig. 7 is 10 corresponding to an effective ratio of L_{ds}/L_{qs} of about 7.0 for real machines with finite stator leakage inductance.

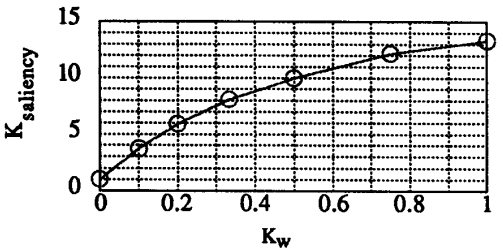

Fig. 7 Saliency ratio $K_{saliency}$ vs. K_w (rotor insulation width/ rotor iron width) resulting from the finite element study of a synchronous reluctance motor with 24 stator slots.

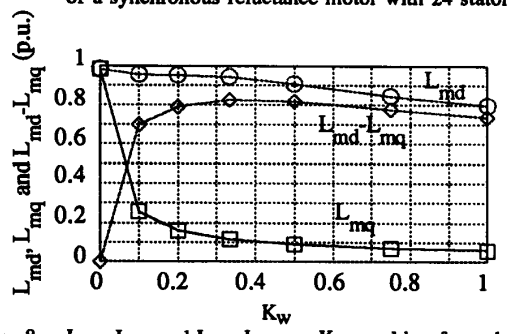

Fig. 8 L_{md}, L_{mq} and L_{md}–L_{mq} vs. K_w resulting from the finite element study of a synchronous reluctance motor with 24 stator slots.

Rotor Design Optimization of Synchronous Reluctance Motor with 36 Stator Slots

While the results shown in the previous section concern only a machine with 24 stator slots having two rotor segments per stator tooth, similar results have been obtained with 36 stator slots and a different number of rotor segments per stator tooth. In this case, the value of n=1 is selected, where n is the number of iron layers of rotor per stator tooth illustrated in Fig. 4. Finite element field plots for the two extreme cases of d-axis and q-axis excitation are shown in Fig. 9. Figure 10 show the air gap flux density as a function of air gap length. Note again that very little flux enters the rotor when the flux is forced to pass through the q-axis, which is similar to Fig. 5 of 24 stator slots case.

The surface current density was again fixed at 500 amperes per inch as the analysis of the motor with 24 stator slots. Specifically, for the case of Figs. 9 and 10, the maximum fundamental component of air gap flux for d-axis excitation obtained from a spectral analysis of the wave form is 0.845 while the fundamental component for q-axis excitation is only 0.085, making the saliency ratio 10 to 1, neglecting the effects of leakage inductance. Note that those obtained values are very close to the fundamental components of the motor with 24 stator slots, i.e., 0.836 and 0.084 for d- and q-axis excitation, respectively.

With a different rotor configuration in which the number of rotor iron-insulation layers is increased as twice as the number of layers of Fig. 9 (increased to n=2), L_{md} is slightly increased by 2.5 % and L_{mq} decreased by 3.5 %, compared with ones in the case of n=1. The harmonic components of the air gap flux density are also improved.

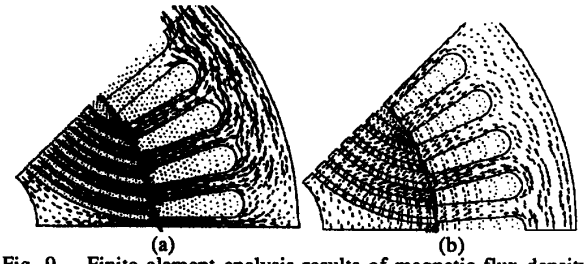

Fig. 9 Finite element analysis results of magnetic flux density distributions of a synchronous reluctance motor with 36 stator slots and K_w (rotor insulation width/ rotor iron width) of 1/2: (a) d-axis excitation, (b) q-axis excitation.

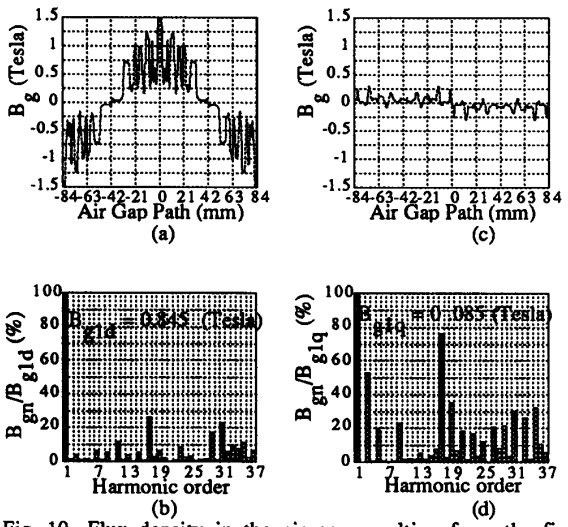

Fig. 10 Flux density in the air gap resulting from the finite element analysis results of a synchronous reluctance motor with 36 stator slots and K_w (rotor insulation width/ rotor iron width) of 1/2: (a) the wave form of the air gap flux density and (b) the harmonic components for d-axis excitation; (c) the wave form of the air gap flux density and (d) the harmonic components for q-axis excitation.

Summary of Rotor Design Optimization of Synchronous Reluctance Motor

Figure 11 shows two curves of L_{md}-L_{mq} versus K_w (rotor insulation width/ rotor iron width) for two different stator-rotor configurations. The figure indicates that the L_{md}–L_{mq} characteristic is quite independent of the stator configuration. The results suggest that K_w has a range of 0.2 to 0.6 for good torque production.

Figure 12 shows two curves of saliency ratio $K_{saliency}$ versus K_w (rotor insulation width/ rotor iron width) for two different stator-rotor configurations. The figure indicates that the saliency ratio is independent of the stator-rotor configuration but dependent on the ratio of the rotor insulation width to the rotor iron width.

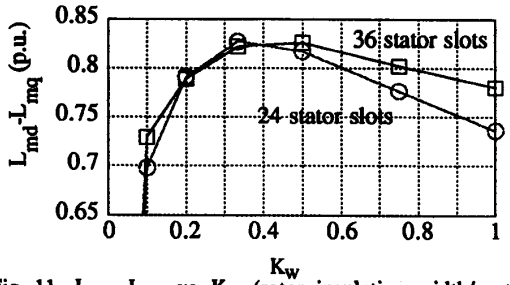

Fig. 11 L_{md}–L_{mq} vs. K_w (rotor insulation width/ rotor iron width) resulting from the finite element study of two different stator-rotor configurations of synchronous reluctance motors.

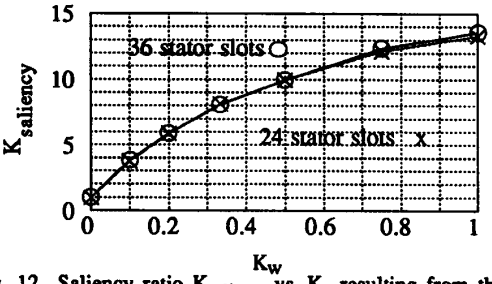

Fig. 12 Saliency ratio $K_{saliency}$ vs. K_w resulting from the finite element study of two different stator-rotor configurations of synchronous reluctance motors.

EXPERIMENTAL SYNCHRONOUS RELUCTANCE MOTOR

An experimental synchronous reluctance motor with 4 poles and 24 stator slots was fabricated to verify the discussions and analysis on the rotor design optimization, where the rotor geometric parameter K_w of 0.5 was chosen. The rated output power of the motor is 300 watts and the air gap, outer and inner stator diameter and stack length are 0.3 mm, 121.7 mm, 68.2 mm and 50.8 mm, respectively.

Finite Element Analysis of The Experimental Synchronous Reluctance Motor

Figure 13 (a) is a plot of d-axis magnetizing inductance calculated from the air gap flux densities obtained from the finite element analysis of the experimental synchronous reluctance motor with d-axis excitation of 0.25 p.u. to 1.5 p.u. and no q-axis current. The d-axis magnetizing inductance L_{md} has been per unitized to the value of L_{md} for i_d=1.0 p.u.

The effects of the existing of the q-axis current on the d-axis magnetizing inductance is shown in Fig. 13 (b) with d-axis excitation of 0.5 p.u., 1.0 p.u., 1.25 p.u., and 1.5 p.u. under the existence of the q-axis current of 0.0 p.u., 0.5 p.u., and 1.5 p.u. Note that only a very small effect on the d-axis magnetizing inductance by the q-axis excitation is observed, i.e., only a few fractional percent of L_{md} decreases due to the q-axis current of 1 p.u.

Figure 14 (a) is a plot of q-axis magnetizing inductance with q-axis excitation of 0.25 p.u. to 1.5 p.u. and no d-axis excitation. The q-axis magnetizing inductance L_{mq} is also per unitized to the value of L_{md} for i_d = 1.0 p.u.. Note that no saturation effect on L_{mq} is observed even for 1.5 p.u. q-axis excitaion as expected.

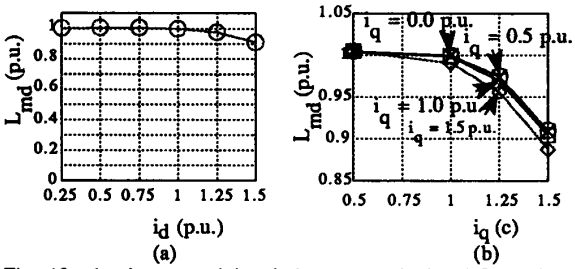

Fig. 13 d-axis magnetizing inductance calculated from the air gap flux densities obtained from the finite element analysis of the designed synchronous reluctance motor : (a) with d-axis excitation of 0.25 p.u. to 1.5 p.u. and no q-axis excitation, (b) with d-axis excitation of 0.5 p.u.,1.0 p.u., 1.25 p.u., and 1.5 p.u. under the conditions of q-axis excitation of 0.0 p.u., 0.5 p.u., 1.5 p.u..

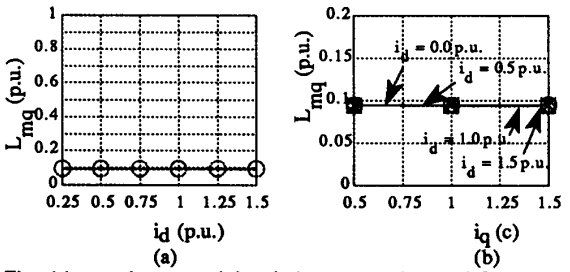

Fig. 14 q-axis magnetizing inductance calculated from the air gap flux density obtained from the finite element analysis of the designed synchronous reluctance motor: (a) with q-axis excitation of 0.25 p.u. to 1.5 p.u. and no d-axis excitation, (b) with q-axis excitation of 0.5 p.u.,1.0 p.u., and 1.5 p.u. under the conditions of d-axis excitation of 0.0 p.u., 0.5 p.u., 1.5 p.u..

The effects of the existing of the d-axis excitation on the q-axis magnetizing inductance is shown in Fig. 14 (b) with q-axis excitation of 0.5 p.u., 1.0 p.u. and 1.5 p.u. under the existence of the d-axis current of 0.0 p.u., 0.5 p.u., 1.0 p.u. and 1.5 p.u. Note that no effect on the d-axis magnetizing inductance by the q-axis excitation is observed.

A very desirable inductance property is clearly obtained for the experimental synchronous reluctance motor. The control of the motor can be significantly simplified since almost no cross coupling effects between d- and q-axis excitations exist.

At the rated conditions, the peak value of the d-axis fundamental component of the air gap flux density is 0.538 Tesla, while the corresponding q-axis component is 0.127 Tesla. Hence, the resulting saliency ratio is 10.6 at the rated condition, neglecting the effects of leakage inductance.

Measurements of Motor Parameters

The inductance L_{ds} and L_{qs} of the experimental synchronous reluctance motor were measured with the single phase ac variable voltage source. The 60 Hz voltage source was applied between the phase a terminal and the phase b terminal with the phases b and c terminal connected together. The inductances were calculated from the obtained results of the measurements using the measured stator resistance. The measured d-axis inductance L_{ds} was 0.102 henries with d-axis excitation of 1 p.u. and 0.107 henries with d-axis excitation of 0.25 p.u., and the measured q-axis inductance L_{qs} was

0.016 henries with q-axis excitation of 0.25 p.u. to 1 p.u. Hence, the saliency ratio of the motor is 6.7 for the unsaturated conditions and 6.4 for the saturated conditions.

The stator leakage inductance L_{ls} was measured under the condition where the rotor was removed from the stator. Although the exact value cannot be obtained under this condition, it is on the low side which results in our prediction of saliency ratio to be on the conservative side. The measured leakage inductance was 0.0077 henries. The d- and q-axis magnetizing inductances, L_{md} and L_{mq}, which can be estimated from the measured inductances, are 0.0943 and 0.0083 henries, respectively. Hence, the saliency ratio L_{md}/L_{mq} is calculated as high as 11.3, which is well matched with the value that was obtained from the finite element study.

CONCLUSIONS

It has been demonstrated in this paper that there is an optimal value for two key geometric variables of the rotor of the synchronous reluctance motor, W_{iron} and W_{ins}, corresponding to the width of each rotor segment and of the width of the insulation between segments, respectively. The ratio of two variables K_w (W_{ins}/W_{iron}) of 0.5 is a near optimal selection. It is also demonstrated by the finite element study that the saliency ratio L_{md}/L_{mq} in the neighborhood of 10 is a realizable value. With reasonably low leakage inductances, the saliency ratio L_{ds}/L_{qs} of 7-8 can be expected, which enables the synchronous reluctance machines with the motor power factor of about 0.8 to be competitive with the induction motors for ac drive applications.

An experimental synchronous reluctance motor was designed and built to verify the discussions and analysis in this paper. The finite element study has shown that the experimental motor has a saliency ratio L_{md}/L_{mq} of 10.6 and very small saturation effects and almost no cross coupling effects were observed on both d- and q-axis magnetizing inductances. The results of the measurements of the experimental synchronous reluctance motor have verified the validity of the rotor design optimization of the synchronous reluctance motor.

ACKNOWLEDGMENT

The authors are grateful to Gary E. Horst of Emerson Electric Co., St. Louis for the fabrication of the experimental synchronous reluctance motor

REFERENCES

[1] T. Matsuo, T. A. Lipo, "A rotor Parameter Identification Scheme for Vector-Controlled Induction Motor Drives", IEEE Transactions on Industry Applications, Volume IA-21, Number 3, May/June 1985, pp. 624-632.

[2] T. A. Lipo, "Synchronous Reluctance Machines - A Viable Alternative for AC Drives?", Electric Machines and Power Systems, 1991, pp. 659-671.

[3] J. K. Kostko, "Polyphase Reaction Synchronous Motors", Journal of American Institute of Electrical Engineers, 1923, 42, pp. 1162-1168.

[4] P. J. Lawrenson and S. K. Gupta, "Developments in the Performance and Theory of Segmental-Rotor Reluctance Motors", Proceedings IEE, Vol. 114, No. 5, May 1967, pp. 645-653.

[5] A. J. O. Cruickshank, A. F. Anderson, R. W. Menzies, "Theory and Performance of Reluctance Motors With Axially Laminated Anisotropic Rotors", Proceedings IEE, Vol. 118, No. 7, July 1971, pp. 887-894.

[6] R. H. Park, "Two-Reaction Theory of Synchronous Machines-II", AIEE Transactions, June 1933.

[7] T. A. Lipo, "Electromagnetic Design of Electric Machines", Class Notes for ECE 713, ECE Department, University of Wisconsin-Madison, 1986.

[8] D. A. Staton, T. J. E. Miller and S. E. Wood, "Optimization of The Synchronous Reluctance Motor Geometty", Electrical Machines and Drives Conference Record, London, UK, 1991, pp. 156-160.

[9] I. Boldea, Z. X. Fu and S. A. Nasar, "Performance Evaluation of Axially-Laminated Anisotropic (ALA) Rotor Reluctance Synchronous Motors", IEEE IAS Annual Meeting Conference Record, 1992, pp. 212-218.

Takayoshi Matsuo (S' 90) was born in Himeji, Japan. He received the B. E. degree in Electrical Engineering and the M. E. degree in Applied Electronics from Tokyo Institute of Technology, Tokyo, Japan, and the M. S. degree in Electrical Engineering from the University of Wisconsin-Madison in 1975 and 1977, and 1983, respectively. From 1977 to 1989 he was an electrical engineer in the Power Electronics Department of the Mitsubishi Electric Corporation, Japan. Since 1989, he has been a research assistant and pursuing the Ph.D. degree in the Department of Electrical and Computer Engineering of the University of Wisconsin-Madison. His research interest is in ac drives, power electronics and electrical machines.

Thomas A. Lipo (M'64-SM'71-F'87) is a native of Milwaukee Wisconsin. He received his B.E.E. and M.S.E.E. degrees from Marquette University, Milwaukee, WI in 1962 and 1964 respectively and the Ph.D. degree in electrical engineering from the University of Wisconsin in 1968. From 1969 to 1979 he was an Electrical Engineer in the Power Electronics Laboratory of Corporate Research and Development of the General Electric Company, Schenectady NY. He became Professor of Electrical Engineering at Purdue University in 1979 and in 1981 he joined the University of Wisconsin in the same capacity. He is presently the W.W. Grainger Professor of Power Electronics and Electrical Machines. He also serves as Co-Director of the Wisconsin Electric Machines and Power Electronics Consortium (WEMPEC) and Director of the Wisconsin Power Electronic Research Center (WisPERC).